

## Polaron spin states in chiral systems

Zi-Wu Wang <sup>1,\*</sup>, Ran-Bo Yang,<sup>1</sup> Yu Cui,<sup>1</sup> Wei-Ping Li,<sup>2</sup> Xiao-Qi Dong,<sup>1</sup> and Zhi-Qing Li<sup>1</sup>

<sup>1</sup>Tianjin Key Laboratory of Low Dimensional Materials Physics and Preparing Technology, Department of Physics, Tianjin University, Tianjin 300354, China

<sup>2</sup>Department of Basic Courses, Tianjin Sino-German University of Applied Sciences, Tianjin 300350, China



(Received 21 January 2024; revised 24 July 2024; accepted 19 August 2024; published 27 August 2024)

We theoretically study polaron spin states in chiral systems for both weak and strong electron-phonon coupling using the well-known Lee-Low-Pines unitary transformations, where the strain tensor induced by the phonon displacement of chiral structures couples directly with the electron spin. We find that the splitting magnitudes of polaron spin states are enlarged significantly with increasing the cutoff wave vector of phonon modes, which directly relate to several key ingredients of the polaron transport for chirality-induced spin selectivity (CISS), such as the lifetime of spin filtering and the effective masses of spin states. These results not only provide a potential CISS mechanism based on direct spin-phonon coupling, but also enrich fundamental physics of polaron studies in various chiral systems.

DOI: [10.1103/PhysRevB.110.085430](https://doi.org/10.1103/PhysRevB.110.085430)

### I. INTRODUCTION

Chirality-induced spin selectivity (CISS), that electron transmission or transport through the chiral molecules has one preferential spin orientation over the other one, was initially discovered in 1999 [1]. From then on, this effect has been proved widely by large numbers of experiments in various chiral systems [2–8], including both the organic and inorganic materials, even some chiral organic-inorganic assemblies. On the one hand, it has been proposed as a testing ground for novel phenomena in quantum physics, chemistry, and biology, such as the unconventional superconductor [2,3,7], enantiomer separations [4,5], and biorecognition [6]. On the other hand, it represents the controllable level of spin degrees of freedom imposing potential applications on quantum sensors, spintronic nanodevices, and quantum information processing [8]. However, a complete quantitative theory to explain CISS remains elusive [9–11] and the microscopic processes are insufficiently understood.

In recent years, polaron transmission and transport instead of the electron in CISS has attracted more attention, because the propagating process in the chiral structures is not an isolated one, as an electron inevitably couples with its surrounding lattice vibrations (phonons) [12–18]. Namely, the formation of the spatial localized polaron is closer to the realistic environment. Several polaron transport models based on spin-orbit coupling, therefore, have been proposed for CISS. For instance, Zhang *et al.* [15] pointed out that the polaron transport through the chiral molecule exhibits a spin-momentum-locked feature and found that just the interplay of the electron-phonon coupling and spin-orbit coupling results in the spin and lattice being coupled, which leads to a strongly enhanced spin coherence and then a very high spin polarization. Fransson [14] predicted that the cooperation of electron-phonon and spin-orbit interactions generates an exchange splitting between the spin channels which is viable

for CISS, which was further confirmed by Vittmann *et al.* [17]. Recently, Klein and Michaeli [18] developed a general framework for calculating polaron transport signatures of CISS in the presence of strong electron-phonon coupling, where polaron fluctuations will result in strong signals of CISS for both spin-dependent scattering and asymmetric magnetoresistance. These polaron models not only give significant enhancement for the spin-orbit coupling that is necessary for large spin polarization, but also provide a reasonable explanation for the temperature dependence of spin polarization in CISS. However, studies for the underlying origin of polaron spin states within chiral systems, to our knowledge, are still at the embryonic stage.

In the present paper, we study polaron spin states in chiral systems based on direct spin-phonon coupling [19–21], in which an elastic strain tensor with chirality is induced by the anisotropic phonon displacement field [22–24]. The ground energies of polaron spin states are obtained by the well-known Lee-Low-Pines (LLP) unitary transformation [25–27]. We present the dependence of the phonon wave vectors on the energy splitting of polaron spin states and find that the splitting magnitudes of spin states depend on the chirality of the hosting systems, which implies that an electron has spin preference during transmission or transport through these chiral structures. These results highlight the crucial roles of the polaron effect on the underlying mechanisms of CISS. Meanwhile, this simple model opens up avenues for studying polaron physics in chiral molecules and structures.

### II. THEORETICAL MODEL

The Hamiltonian of a polaron with different spin states in the system of spin-phonon coupling can be written as [19–21]

$$H = \frac{P^2}{2m^*} + \sum_k \hbar\omega_0 a_k^\dagger a_k + \frac{v}{2} \sigma_z (\xi_{zx} P_x - \xi_{zy} P_y), \quad (1)$$

where the first term describes the momentum energy for an electron with the effective mass  $m^*$  and the momentum  $P$ . The

\*Contact author: wangziwu@tju.edu.cn

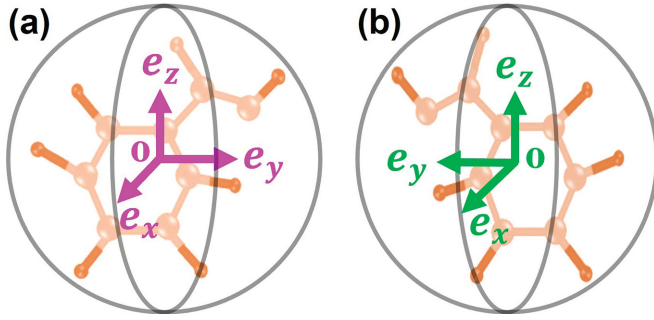


FIG. 1. Schematic diagrams of chiral systems, where three components ( $\mathbf{e}_x$ ,  $\mathbf{e}_y$ ,  $\mathbf{e}_z$ ) of the phonon displacement field are assumed for the left-handed (a) and right-handed (b) molecules. This phonon displacement induces the chiral strain tensor coupling with the electron spin directly.

second term stands for the energy of the phononic bath with an average frequency  $\omega_0$ , and  $a_k$  ( $a_k^\dagger$ ) is an annihilation (creation) operator of the phonon with the wave vector  $k$ . The third term denotes the direct coupling between the spin states of the electron and the phonon modes with a phenomenological coupling constant  $\nu$ , and  $\sigma_z$  is the Pauli matrix with the eigenvalues  $\pm 1$ , representing the spin-up and -down states, respectively.  $\xi_{zx}$  and  $\xi_{zy}$  are the components of the lattice strain tensor [19–23]:

$$\xi_{zx} = \frac{1}{2} \left\{ \frac{\partial U_x}{\partial z} + \frac{\partial U_z}{\partial x} \right\}, \quad (2a)$$

$$\xi_{zy} = \frac{1}{2} \left\{ \frac{\partial U_y}{\partial z} + \frac{\partial U_z}{\partial y} \right\}, \quad (2b)$$

which are induced by the phonon displacement field

$$U = \sum_k \left[ \frac{\hbar}{2\rho\omega_0} \right]^{\frac{1}{2}} (a_k e^{i\mathbf{k}\cdot\mathbf{r}} + a_k^\dagger e^{-i\mathbf{k}\cdot\mathbf{r}}) \mathbf{e}_{m=x,y,z}, \quad (3)$$

where  $\rho$  is the mass density and  $\mathbf{e}_{m=x,y,z}$  is the phonon polarization. The relations of the effective phonon displacement fields with the chiral geometry of molecules or structures are illustrated in Fig. 1 [24]. The detailed expressions for the elastic strain can be given by

$$\xi_{zx} = \sum_k [V_{zx} a_k e^{i\mathbf{k}\cdot\mathbf{r}} + V_{zx}^* a_k^\dagger e^{-i\mathbf{k}\cdot\mathbf{r}}], \quad (4a)$$

$$\xi_{zy} = \sum_k [V_{zy} a_k e^{i\mathbf{k}\cdot\mathbf{r}} + V_{zy}^* a_k^\dagger e^{-i\mathbf{k}\cdot\mathbf{r}}], \quad (4b)$$

with the chiral coupling parameters

$$V_{zx}^R = i \left[ \frac{\hbar}{2\rho\omega_0} \right]^{\frac{1}{2}} [k_z(\mathbf{e}_x) + k_x(\mathbf{e}_z)], \quad (5a)$$

$$V_{zy}^R = i \left[ \frac{\hbar}{2\rho\omega_0} \right]^{\frac{1}{2}} [k_z(\mathbf{e}_y) + k_y(\mathbf{e}_z)] \quad (5b)$$

for the right-handed structures and

$$V_{zx}^L = i \left[ \frac{\hbar}{2\rho\omega_0} \right]^{\frac{1}{2}} [k_z(\mathbf{e}_x) + k_x(\mathbf{e}_z)], \quad (6a)$$

$$V_{zy}^L = i \left[ \frac{\hbar}{2\rho\omega_0} \right]^{\frac{1}{2}} [k_z(\mathbf{e}_y) - k_y(\mathbf{e}_z)] \quad (6b)$$

for the left-handed ones.

Within the LLP model [25–27], the first and second unitary transformations are

$$W_1 = \exp \left( -i \sum_k k r a_k^\dagger a_k \right), \quad (7a)$$

$$W_2 = \exp \left[ \sum_k (f_k a_k^\dagger - f_k^* a_k) \right], \quad (7b)$$

respectively, with  $f_k$  ( $f_k^*$ ) the variational parameter. Substituting Eqs. (7a) and (7b) into the polaron's Hamiltonian, and then performing the LLP transformation, the transformed Hamiltonian is

$$\tilde{H} = W_1^{-1} W_2^{-1} H W_2 W_1 \approx \tilde{H}_0 \quad (8)$$

and

$$\begin{aligned} \tilde{H}_0 = & \frac{p^2}{2m^*} + \sum_k \left( \hbar\omega_0 + \frac{\hbar^2 k^2}{2m^*} \right) (a_k^\dagger + f_k^*) (a_k + f_k) \\ & + \frac{\nu}{2} \sigma_z \sum_k (V_{zy}^{(j)} \hbar k_y - V_{zx}^{(j)} \hbar k_x) (a_k + f_k) \\ & + \sum_k (V_{zx}^{*(j)} \hbar k_x - V_{zy}^{*(j)} \hbar k_y) (a_k^\dagger + f_k^*), \end{aligned} \quad (9)$$

where some terms including interaction between different phonons modes, such as two-phonon process with different wave vectors, have been neglected in the transformation processes because of the tiny correction to the total energy of the polaron.. The superscripts  $j = R, L$  denote the right- and left-handed structures, respectively. The trial wave function of the Hamiltonian  $\tilde{H}_0$  for the ground state of the polaron [26,27]

$$|\psi\rangle = |e^{iQr}\rangle |0_{\text{ph}}\rangle |\chi_z\rangle, \quad (10)$$

where  $|e^{iQr}\rangle$  is the eigenfunction of the electronic state with the wave vector  $Q$ ,  $|0\rangle_{\text{ph}}$  denotes the zero phonon state, and  $\chi_z$  is the wave function of the spin state with the eigenvalues  $\pm 1$ , representing the spin-up ( $\uparrow$ ) and spin-down ( $\downarrow$ ) states, respectively. The expectation values of the energies for polaron spin states can be obtained via

$$\begin{aligned} E_{\uparrow,\downarrow}^{(j)} = \langle \psi | \tilde{H}_0 | \psi \rangle = & \frac{\hbar^2 Q^2}{2m^*} + \sum_k \left( \hbar\omega_0 + \frac{\hbar^2 k^2}{2m^*} \right) f_k^* f_k \\ & \pm \frac{\nu}{2} \sum_k (V_{zy}^{(j)} \hbar k_y - V_{zx}^{(j)} \hbar k_x) f_k \\ & \pm \sum_k (V_{zx}^{*(j)} \hbar k_x - V_{zy}^{*(j)} \hbar k_y) f_k^*, \end{aligned} \quad (11)$$

where the relations  $a_k |0_{\text{ph}}\rangle = 0$  and  $a_k^\dagger |0_{\text{ph}}\rangle = |1\rangle$  are applied. Minimizing Eq. (11) with respect to  $f_k$  and  $f_k^*$ , we get

$$f_k^{(j)} = \mp \frac{\nu (V_{zy}^{*(j)} \hbar k_y - V_{zx}^{*(j)} \hbar k_x) / 2}{\hbar^2 k^2 / (2m^*) + \hbar\omega_0}, \quad (12a)$$

$$f_k^{*(j)} = \mp \frac{\nu (V_{zy}^{(j)} \hbar k_y - V_{zx}^{(j)} \hbar k_x) / 2}{\hbar^2 k^2 / (2m^*) + \hbar\omega_0}. \quad (12b)$$

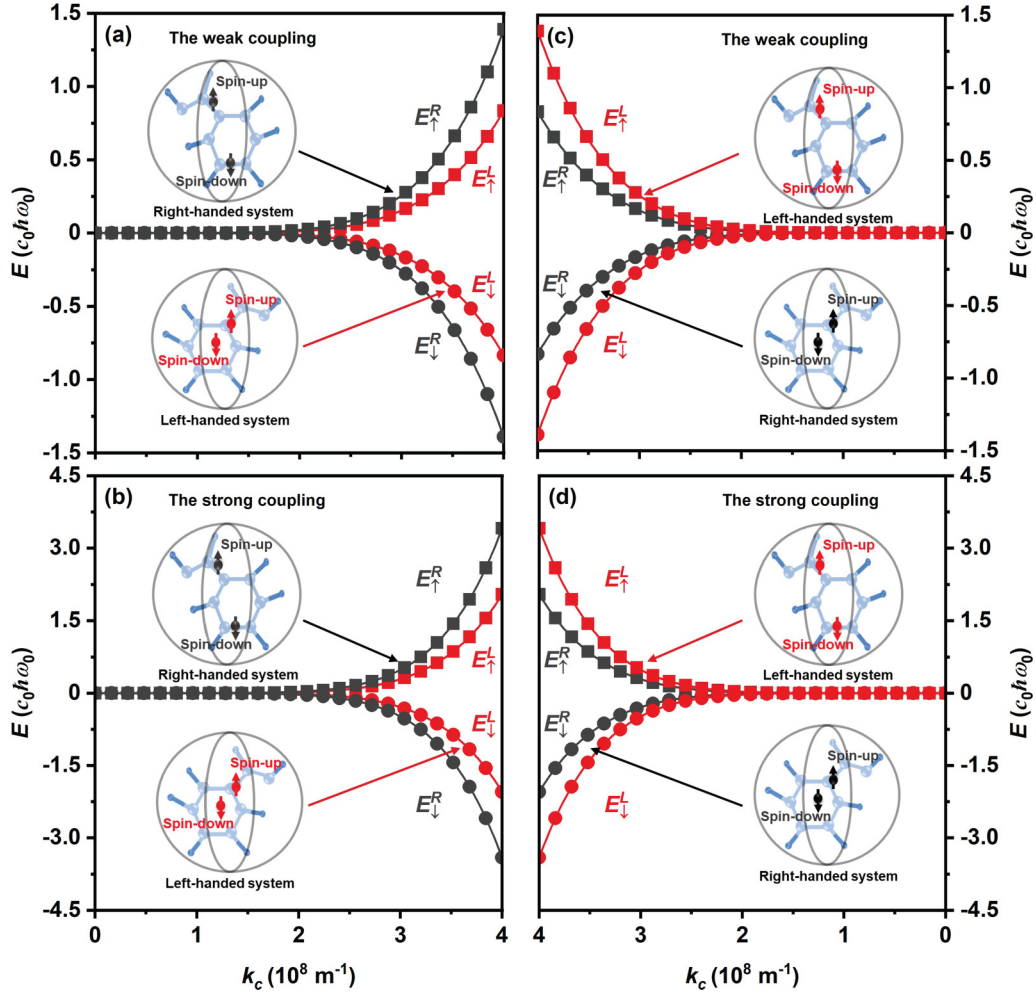


FIG. 2. (a), (b) The energy splitting of polaron spin states as a function of the phonon wave vectors for the right- and left-handed structures with weak (a) and strong (b) electron-phonon coupling. (c), (d) The opposite distributions of spin states when electrons move in the opposite direction, compared to those in (a) and (b), respectively, where the constant  $c_0 = \xi_0 / (\hbar\omega_0 m^7)$ .

Substituting Eqs. (12a) and (12b) into Eq. (11), we get the ground energies of polaron spin states:

$$E_{\uparrow,\downarrow}^{(R)} = \pm \xi_0 \sum_k \frac{[k_x^2(k_x^2 + k_z^2) + k_y^2(k_y^2 + k_z^2) + 2k_x^2 k_y^2]}{\hbar^2 k^2 / (2m^*) + \hbar\omega_0} \quad (13)$$

for the right-handed structure and

$$E_{\uparrow,\downarrow}^{(L)} = \pm \xi_0 \sum_k \frac{[k_x^2(k_x^2 + k_z^2) + k_y^2(k_y^2 + k_z^2) - 2k_x^2 k_y^2]}{\hbar^2 k^2 / (2m^*) + \hbar\omega_0} \quad (14)$$

for the left-handed structure, respectively, where  $\xi_0 = v^2 \hbar^3 / (8\rho\omega_0)$  and  $P \equiv Q = 0$  are adopted for the ground state of the polaron in Eqs. (13) and (14). In fact, the method of two-unitary transformation has been extensively employed in traditional polaron physics for weak electron-phonon coupling. For the strong-coupling case, only the second unitary transformation is carried out for the polaron's Hamiltonian [26,27], which is also an advantage of this method. Following similar processes of the weak-coupling case mentioned above, we can easily get the expressions of the variational function  $f_k^{(j)}$  ( $f_k^{*(j)}$ ) and the ground energies of polaron  $E_{\uparrow,\downarrow}^{(j)}$  for the strong-coupling case (see the

Appendix). Converting the summation of phonon wave vector  $k$  into the integral  $\sum_k = 1/(2\pi)^3 \int_0^{k_c} k^2 dk \int_0^\pi \sin\theta d\theta \int_0^{2\pi} d\varphi$  for Eqs. (13) and (14), one can get the splitting of polaron spin states for the weak- and strong-coupling cases as shown in Fig. 2, where  $k_c$  denotes the cutoff wave vector for the phonon mode.

### III. RESULTS AND DISCUSSION

Figure 2(a) displays the energy splitting of polaron spin states as a function of the cutoff wave vector of phonon modes for the right- and left-handed structures in the weak-coupling case. One can see that the amplitudes of spin splitting are enlarged markedly with an increasing of the phonon wave vector. This implies that the shorter the wavelength of phonon modes (corresponding to a bigger phonon wave vector) the stronger the coupling to the electron spin. In the present paper, the displacement field of the acoustic phonon modes via the deformation mechanism is assumed arising from the facts that (i) the lattice and molecular deformation (distortion) are very common and even inevitable for most organic materials due to the origin of the soft lattice [5,13,23] and (ii) chiral molecules laying on the ferromagnetic or metal

substrates result not only in the deformation being enhanced significantly, but also in the local interface phonon modes being induced, giving an additional coupling contribution to electron spin in most experiments [2–6]. On the other hand, optical phonon modes via the deformation mechanism in chiral structures should also contribute a similar effect to the spin splitting. In particular, certain types of deformation optical phonon modes strongly couple with electrons, leading to the formation of strong-coupling polarons in traditional semiconductors [26,27]. This will give rise to much larger spin splitting as shown in Fig. 2(b) in the strong-coupling case. In addition, it can be easily inferred from Eqs. (12) and (13) that the splitting amplitude will be enhanced significantly with increasing the coupling constant  $\nu$  included in the spin-phonon coupling term, which denotes the velocity of the phonon mode and could be varied in the large scale when different types of phonon modes are taken into account. Therefore, the CISS effect may be enlarged efficiently by the spin-phonon coupling except for a fundamental mechanism based on a coupling of electron spin with the chiral structure mediated by spin-orbital interaction [4,28]. In Figs. 2(a) and 2(b), we only present the distribution of spin states when electrons move in one direction through right- and left-handed structures, respectively. When electrons move in the opposite direction, one can see that the opposite distributions of spin states appear as shown in Figs. 2(c) and 2(d).

In addition to polaron transport instead of electron transport in CISS, several phonon-assisted CISS mechanisms that highlight the crucial roles of phonon modes of chiral structures have also been proposed. For instance, electron spin dynamics in a deformable helical molecule was studied and shows that just the electron-phonon coupling ensures the formation of stable solitons with the preferred spin projection onto the molecule axis [12]. The influences of electron-vibration interaction on the spin-selective transport in double-stranded DNA molecules were investigated, where not only the spin polarization is enhanced, but also a series of new spin-splitting transmission modes are induced by the electron-lattice interaction [13]. The nonequilibrium dynamics of delocalized phonon modes of chiral molecules induce the fluctuation of the spin-orbit coupling when an electron is propagating through helical potentials, enhancing the spin selectivity [14]. Obviously, the present model shows a microscopic origin that phonon modes of chiral structure induce the chiral strain tensor, leading to the difference of spin splitting and thus spin selectivity. Meanwhile, a potential CISS mechanism based on direct spin-phonon coupling is proposed, compensating for the weak spin-orbital coupling in chiral materials in previous models. On the other hand, the temperature dependence of spin polarization has been widely studied in experiments, where different trends including positive [29–31] and negative [2] dependence and even independence [32] were obtained. Hence, the temperature dependence of CISS needs to be explored further. Polaron states describing an electron dressed by the surrounding lattice phonons provide a potential explanation for the temperature dependence of CISS, because the temperature directly relates to the average phonon numbers around a polaron [26,27].

Although the coupling between the electron spin and phonon field plays an important role in CISS as mentioned

above, the underlying microscopic mechanism should be the synergistic effect of many elements of the chiral structures, such as the electron-electron correlation [14], the interface-induced momentum conservation [33], the interplay between friction and spin-orbit coupling [34], the anisotropic effect of dipole moments of chiral molecules [24], and the substantial perturbation in the presence of accidental degeneracies in the molecular spectrum [35].

Here, the direct spin-phonon coupling mechanism is used to analyze the splitting of polaron spin states in chiral systems, which, in fact, was originally developed for studying the spin-flip relaxation for the spin dynamics in semiconductors [20,21] and has been expanded to related problems in many low-dimensional materials [36–38]. From the discrepancy of the splitting magnitude of spin states in chiral systems shown in Fig. 2, it can be predicted that several key ingredients of polaron transport depend on the chirality of these structures directly. For instance, the mobility of a polaron  $\mu = e\tau/m^*$  [25] with average scattering time with spin flipping  $\tau \propto (2\pi/\hbar)|H'|^2\delta(E_{\uparrow}^j - E_{\downarrow}^j)$  [20,21] and the effective mass of a polaron  $m^{*j} \propto m^*/[1 \pm s\sqrt{2E^j/(m^*\nu^2)}]$  [26,27] are related to the energy splitting of spin states ( $s = \uparrow, \downarrow$ ) and the chirality of system ( $j = L, R$ ). These two physical parameters have been extensively studied by many traditional methods in experiments [26,27,39], which implies that these experimental methods could also be used to identify the CISS effect.

In addition, we only adopt a very simple and traditional method to study polaron physics in this paper. In the past several decades, many advanced methods have been developed to study the polaron effect, such as diagrammatic quantum Monte Carlo method, Feynman path integral method, and first-principles calculation based on the density functional theory [39,40]. Therefore, we hope our results will stimulate these advanced methods to explore polaron states in chiral systems and even the progress of related experiments.

#### IV. CONCLUSION

In summary, we study the polaron effect of spin states in chiral systems using the well-known Lee-Low-Pines variational method. We show that (i) chiral geometry intrinsically induces the discrepancy of spin-phonon coupling, characterized by the different splitting magnitudes of polaron spin states, which highlights not only polaron transport but that the electron spin couples with the chiral frame; and (ii) the splitting magnitudes of polaron spin states are enlarged significantly with increasing the cutoff wave vector of phonon modes, implying that the CISS effect could be effectively magnified by phonon displacement of the chiral structure. These theoretical results enlighten the exploration of phonon-assisted CISS mechanisms.

#### ACKNOWLEDGMENTS

This work was supported by National Natural Science Foundation of China (Grants No. 12164032 and No. 12174283), Natural Science Foundation of Tianjin Sino-German University of Applied Science (Grant No. ZDKT2016-003), and University-Level Research Project of

Tianjin Sino-German University of Applied Sciences (Grant No. ZDKT2018-007).

### APPENDIX: VARIATIONAL FUNCTIONS AND EIGENFUNCTIONS FOR POLARON SPIN STATES WITH STRONG COUPLING

Within the frame of LLP's polaron model [25–27], the variational functions  $f_k$  and  $f_k^*$  in the strong-coupling case can be expressed as

$$f_k^{(j)} = \mp \frac{v(V_{zy}^{*(j)} \hbar k_y - V_{zx}^{*(j)} \hbar k_x) \exp(-r_0^2 k^2/4)}{2\hbar\omega_0}, \quad (\text{A1a})$$

$$f_k^{*(j)} = \mp \frac{v(V_{zy}^{(j)} \hbar k_y - V_{zx}^{(j)} \hbar k_x) \exp(-r_0^2 k^2/4)}{2\hbar\omega_0}, \quad (\text{A1b})$$

where  $r_0 = \sqrt{\hbar/(m^*\omega_0)}$  denotes the radius of the polaron ( $r_0=1.5$  nm is adopted in the numerical simulation). Following a similar process for the weak-coupling case mentioned above, the ground energies of polaron spin states for the strong-coupling case can be written as

$$E_{\uparrow,\downarrow}^{(R)} = \pm \xi_0 \sum_k \frac{[k_x^2(k_x^2 + k_z^2) + k_y^2(k_y^2 + k_z^2) + 2k_x^2 k_y^2] \Omega(k)}{\hbar\omega_0} \quad (\text{A2})$$

for the right-handed structure and

$$E_{\uparrow,\downarrow}^{(L)} = \pm \xi_0 \sum_k \frac{[k_x^2(k_x^2 + k_z^2) + k_y^2(k_y^2 + k_z^2) - 2k_x^2 k_y^2] \Omega(k)}{\hbar\omega_0} \quad (\text{A3})$$

for the left-handed structure. Here,  $\Omega(k) = \exp(-r_0^2 k^2/2)$ .

- [1] K. Ray, S. P. Ananthavel, D. H. Waldeck, and R. Naaman, Asymmetric scattering of polarized electrons by organized organic films made of chiral molecules, *Science* **283**, 814 (1999).
- [2] R. Naaman and D. H. Waldeck, Spintronics and chirality: Spin selectivity in electron transport through chiral molecules, *Annu. Rev. Phys. Chem.* **66**, 263 (2015).
- [3] R. Naaman, Y. Paltiel, and D. H. Waldeck, Chiral molecules and the electron spin, *Nat. Rev. Chem.* **3**, 250 (2019).
- [4] R. Naaman, Y. Paltiel, and D. H. Waldeck, Chiral molecules and the spin selectivity effect, *J. Phys. Chem. Lett.* **11**, 3660 (2020).
- [5] D. H. Waldeck, R. Naaman, and Y. Paltiel, The spin selectivity effect in chiral materials, *APL Mater.* **9**, 040902 (2021).
- [6] R. Naaman, Y. Paltiel, and D. H. Waldeck, Chiral induced spin selectivity and its implications for biological functions, *Annu. Rev. Biophys.* **51**, 99 (2022).
- [7] F. Evers *et al.*, Theory of chirality induced spin selectivity: Progress and challenges, *Adv. Mater.* **34**, 2106629 (2022).
- [8] A. Chiesa, A. Privitera, E. Macaluso, M. Mannini, R. Bittl, R. Naaman, M. R. Wasielewski, R. Sessoli, and S. Carretta, Chirality-induced spin selectivity: An enabling technology for quantum applications, *Adv. Mater.* **35**, 2300472 (2023).
- [9] J. Fransson, The chiral induced spin selectivity effect what it is, what it is not, and why it matters, *Isr. J. Chem.* **62**, e202200046 (2022).
- [10] S. Alwan, A. Sharoni, and Y. Dubi, Role of electrode polarization in the electron transport chirality induced spin-selectivity effect, *J. Phys. Chem. C* **128**, 6438 (2024).
- [11] B. P. Bloom, Y. Paltiel, R. Naaman, and D. H. Waldeck, Chiral induced spin selectivity, *Chem. Rev.* **124**, 1950 (2024).
- [12] E. Díaz, P. Albares, P. G. Estevez, J. M. Cervero, C. Gaul, E. Diez, and F. D.-Adame, Spin dynamics in helical molecules with nonlinear interactions, *New J. Phys.* **20**, 043055 (2018).
- [13] G.-F. Du, H.-H. Fu, and R. Wu, Vibration-enhanced spin-selective transport of electrons in the DNA double helix, *Phys. Rev. B* **102**, 035431 (2020).
- [14] J. Fransson, Vibrational origin of exchange splitting and chiral-induced spin selectivity, *Phys. Rev. B* **102**, 235416 (2020).
- [15] L. Zhang, Y. Hao, W. Qin, S. Xie, and F. Qu, Chiral-induced spin selectivity: A polaron transport model, *Phys. Rev. B* **102**, 214303 (2020).
- [16] A. Kato, H. M. Yamamoto, and J. Kishine, Chirality-induced spin-filtering in pseudo Jahn-Teller molecules, *Phys. Rev. B* **105**, 195117 (2022).
- [17] C. Vittmann, J. Lim, D. Tamascelli, S. F. Huelga, and M. B. Plenio, Spin-dependent momentum conservation of electron-phonon scattering in chirality-induced spin selectivity, *J. Phys. Chem. Lett.* **14**, 340 (2023).
- [18] D. Klein and K. Michaeli, Giant chirality-induced spin selectivity of polarons, *Phys. Rev. B* **107**, 045404 (2023).
- [19] D. M. Frenkel, Spin relaxation in GaAs-Al<sub>x</sub>Ga<sub>1-x</sub>As heterostructures in high magnetic fields, *Phys. Rev. B* **43**, 14228 (1991).
- [20] A. V. Khaetskii and Y. V. Nazarov, Spin relaxation in semiconductor quantum dots, *Phys. Rev. B* **61**, 12639 (2000).
- [21] A. V. Khaetskii and Y. V. Nazarov, Spin-flip transitions between Zeeman sublevels in semiconductor quantum dots, *Phys. Rev. B* **64**, 125316 (2001).
- [22] T. Yu, Z. Luo and G. E. W. Bauer, Chirality as generalized spin-orbit interaction in spintronics, *Phys. Rep.* **1009**, 1 (2023).
- [23] T. Funato, M. Matsuo, and T. Kato, Chirality-induced phonon-spin conversion at an interface, *Phys. Rev. Lett.* **132**, 236201 (2024).
- [24] A. Ghazaryan, Y. Paltiel, and M. Lemesko, Analytic model of chiral-induced spin selectivity, *J. Phys. Chem. C* **124**, 11716 (2020).
- [25] T. D. Lee, F. E. Low, and D. Pines, The motion of slow electrons in a polar crystal, *Phys. Rev.* **90**, 297 (1953).
- [26] J. T. Devreese, Fröhlich polarons from 0D to 3D: Concepts and recent developments, *J. Phys.: Condens. Matter* **19**, 255201 (2007).
- [27] J. T. Devreese and A. S. Alexandrov, Fröhlich polaron and bipolaron: Recent developments, *Rep. Prog. Phys.* **72**, 066501 (2009).
- [28] J. Fransson, Chirality-induced spin selectivity: The role of electron correlations, *J. Phys. Chem. Lett.* **10**, 7126 (2019).
- [29] T. K. Das, F. Tassinari, R. Naaman, and J. Fransson, Temperature-dependent chiral-induced spin selectivity effect: Experiments and theory, *J. Phys. Chem. C* **126**, 3257 (2022).
- [30] S. Alwan, S. Sarkar, A. Sharoni, and Y. Dubi, Temperature-dependence of the chirality-induced spin selectivity effect: Experiments and theory, *J. Phys. Chem.* **159**, 014106 (2023).

- [31] J. Fransson, Temperature activated chiral induced spin selectivity, *J. Chem. Phys.* **159**, 084115 (2023).
- [32] D.-Y. Zhang, Y. Sang, T. K. Das, Z. Guan, N. Zhong, C.-G. Duan, W. Wang, J. Fransson, R. Naaman, and H.-B. Yang, Highly conductive topologically chiral molecular knots as efficient spin filters, *J. Am. Chem. Soc.* **145**, 26791 (2023).
- [33] C. Vittmann, R. K. Kessing, J. Lim, S. F. Huelga, and M. B. Plenio, Interface-induced conservation of momentum leads to chiral-induced spin selectivity, *J. Phys. Chem. Lett.* **13**, 1791 (2022).
- [34] A. G. Volosniev, H. Alpern, Y. Paltiel, O. Millo, M. Lemesko, and A. Ghazaryan, Interplay between friction and spin-orbit coupling as a source of spin polarization, *Phys. Rev. B* **104**, 024430 (2021).
- [35] S. Dalum and P. Hedegrd, Theory of chiral induced spin selectivity, *Nano Lett.* **19**, 5253 (2019).
- [36] C. L. Romano, G. E. Marques, L. Sanz, and A. M. Alcalde, Phonon modulation of the spin-orbit interaction as a spin relaxation mechanism in quantum dots, *Phys. Rev. B* **77**, 033301 (2008).
- [37] P. R. Struck and G. Burkard, Effective time-reversal symmetry breaking in the spin relaxation in a graphene quantum dot, *Phys. Rev. B* **82**, 125401 (2010).
- [38] G. Burkard, T. D. Ladd, A. Pan, J. M. Nichol, and J. R. Petta, Semiconductor spin qubits, *Rev. Mod. Phys.* **95**, 025003 (2023).
- [39] C. Franchini, M. Reticcioli, M. Setvin, and U. Diebold, Polarons in materials, *Nat. Rev. Mater.* **6**, 560 (2022).
- [40] W. H. Sio and F. Giustino, Polarons in two-dimensional atomic crystals, *Nat. Phys.* **19**, 629 (2023).